JOURNAL OF SOLID STATE CHEMISTRY 60, 41–50 (1985)

The Crystal Structure of Barium Lead Hexaaluminate Phase II

N. IYI, Z. INOUE, S. TAKEKAWA, AND S. KIMURA

National Institute for Research in Inorganic Materials (NIRIM), Namiki 1-1, Sakura-mura, Niihari-gun, Ibaraki, 305, Japan

Received December 10, 1984; in revised form April 2, 1985

A refinement was performed on the average crystal structure of barium lead hexaaluminate phase II ($(Ba_{0.8}Pb_{0.2})_{2.34}Al_{21.0}O_{33.84}$) using single crystal X-ray diffraction data, giving a final R value of 0.030 with space group symmetry $P\bar{6}m2$. The structure is essentially of a β-alumina type, but contains a lot of defects and interstitials. Inside the spinel block were found Ba(Pb) ions at 12-coordinated polyhedral sites, formed by complex defects, including triple Reidinger defects, in the same unit cell. Barium lead hexaaluminate phase II was found to consist of two kinds of unit cells with formulae "$(BaPb)_{3.0}Al_{20.0}O_{35.0}$" and "$Ba_{2.0}Al_{22.0}O_{34.0}$" in a 1 : 2 ratio; these three cells combine to form an $a\sqrt{3} \times a\sqrt{3}$ superstructure.

Introduction

In the $BaO–Al_2O_3$ system, Haberey *et al.* (*1*) found two very similar hexagonal barium aluminates, which previously were considered to be the same compound expressed as "$BaO \cdot 6Al_2O_3$." They were referred to as barium hexaaluminate phase I and phase II by Kimura *et al.* (*2*). At present, the best formulae seem to be $Ba_{0.75}Al_{11}O_{17.25}$ (*3*, *4*), and $Ba_{2.34}Al_{21}O_{33.84}$ (*5*), respectively. In a previous paper (*6*), by using X-ray single crystal diffraction data, we revealed the crystal structure of barium hexaaluminate phase I to be of a β-alumina (β-Al_2O_3) type with the same charge compensation mechanism (*7*) as was found in M^+ β-alumina compounds (M^+: monovalent cations). For this reason barium hexaaluminate phase I was denoted as barium β-alumina. Barium β-alumina was supposed to be made up of two types of half unit cells; "$BaAl_{11}O_{17}$" and "$OAl_{11}O_{17}$" in a 3 : 1 ratio for attaining charge balance. The same structure model was also proposed by van Berkel *et al.* (*4*) independently. Thus the crystal structure and defect nature of barium β-alumina have been clarified. However, the structure of barium hexaaluminate phase II, referred to as barium β(II)-alumina in this paper, remains uncertain. From the chemical formula, electron diffraction data, and the presence of an $a\sqrt{3} \times a\sqrt{3}$ superstructure, we presumed that barium β(II)-alumina would have β-Al_2O_3-like structure with space group symmetry $P\bar{6}$, and we made a preliminary structure model in which conduction layers (mirror planes) alternately consist of a fully occupied Ba–O layer and an excess Ba–O layer (*5*). Later Zandvergen *et al.* (*8*) found "$1.31BaO \cdot 6Ga_2O_3$" to have a similar structure by electron microscopic observation and elaborated our model by considering plausible defect mechanisms. But they presented no definite

0022-4596/85 $3.00

evidence for the model. Though Morgan and Shaw (*9*) and Yamamoto and O'Keeffe (*10*) also observed the $a\sqrt{3} \times a\sqrt{3}$ superstructure for barium β(II)-alumina, they clarified neither the chemical formula nor the basic structure type.

To clarify the crystal structure, it is desirable to obtain single crystals. For barium β-alumina, single crystals were grown by the floating zone (FZ) method (*5*). By the same method, single crystals of barium β(II)-alumina were not obtained. Fortunately, from the PbO–PbF_2 flux, single crystal growth of isostructural barium lead β(II)-alumina was achieved, in which about 20% of the Ba was substituted by Pb ions (*5*).

The object of the present study is to reveal the crystal structure of barium lead β(II)-alumina by X-ray single crystal diffraction, and to clarify the charge compensation mechanism and the causes of the superstructure of barium β(II)-alumina on the basis of the refined parameters.

Experimental

The specimens used for our structural investigation were taken from flux-grown crystals of barium lead β(II)-alumina. PbO–PbF_2 (1 : 1 molar ratio) was used as the solvent and the crystal growth was accomplished under conditions already described (*6, 11*). The chemical formula of the resulting crystal was found to be $(Ba_{0.8}Pb_{0.2})_{2.34}Al_{21.0}O_{33.84}$ by using electron probe microanalysis (EPMA) data, lattice parameters, and density (*5*). Electron microscopy showed that large crystals tended to contain defects of "antiphase boundary (APB)" with displacement vector $\frac{1}{2}c$, which we will discuss in the final section. These crystals were examined also by the precession photographs using Mo$K\alpha$ radiation. Diffuseness perpendicular to c^* axis around (00l) spots (where l = odd) was observed for several large crystals of 0.2-mm order, which may be due to "APB" defects. To avoid the "APB defects," smaller crystals were chosen, and furthermore, a specimen with clear (00l) (where l = odd) spots was selected for X-ray diffraction data collection. The selected hexagonal prism crystal was of dimension 0.05 × 0.05 × 0.08 mm^3. Previously we (*5*) assumed the space group symmetry to be $P\bar{6}$. A preliminary study of Bando (*12*) using the convergent beam electron diffraction (CBED) method indicated the presence of $\bar{6}$ axis. There are two possibilities, either $P\bar{6}$ or $P\bar{6}m2$. So we accomplished the refinement, at first, by assuming $P\bar{6}$ symmetry, and then $P\bar{6}m2$.

The intensities were measured only on the Bragg reflections below $2\theta = 120°$, using a computer-controlled four-circle diffractometer (Rigaku Denki Co., Ltd.) with monochromated Mo$K\alpha$ radiation (λ = 0.71069 Å). A set of (220), (114), and (205) reflections was measured every 50 reflections as standard. The 596 independent nonzero reflections were collected and successively subjected to the Lorenz polarization and absorption corrections. The linear absorption coefficient was μ = 71.6 cm^{-1}; the absorption corrections were applied. Scattering factors were taken from the *International Tables for X-Ray Crystallography* (Vol. 4, 1974) for neutral atoms. For the least-squares refinement, the modified RSFLS-4 program (UNICS) (*13*) was used, and, for Fourier synthesis, RSSFR-5 pro-

TABLE I

CRYSTALLOGRAPHIC DATA[a]

Formula	$(Ba_{0.80}Pb_{0.20})_{2.34}Al_{21.0}O_{33.84}$
Symmetry	Hexagonal
Space group	$P\bar{6}m2$
a	5.6003(5) Å
c	22.922(2) Å
V	622.57(9) Å^3
Z	1
D_{obs}	3.88 gcm^{-3}

[a] For subcell structure.

gram (UNICS) (*14*) was adopted. The lattice parameters were refined using 2θ-data of 19 reflections measured on the four-circle diffractometer. For the similarity to a β-alumina structure, the nomenclature of the cation sites in the mirror plane is after that of Peters *et al.* (*15*). The crystallographic data are shown in Table I with some revisions.

A list of the observed and calculated structure factors is available from the authors.

Refinement

At first, Fourier and difference Fourier syntheses were accomplished using centrosymmetrical β-Al_2O_3 model with full occupancy of Ba at the Beevers-Ross (BR) sites (*15*) because of the similarity of barium lead β(II)-alumina to a β-Al_2O_3 structure. The positional parameters were chosen from those of barium β-alumina (*6*). Coordinates were adjusted to space group $P\bar{6}$ by moving the $z = 0.25$ mirror plane of $P6_3/mmc$ to $z = 0.0$. R value $= \Sigma||F_o| - |F_c||/\Sigma|F_o|$ was 0.287 at this stage. Because the starting model is centrosymmetrical, the resulting Fourier maps were also overlapped with their centrosymmetrical counterparts. These maps showed additional electron densities at ($\frac{2}{3}$, $\frac{1}{3}$, 0.24) and (0.8, 0.2, 0.07) and their centrosymmetrical positions. Furthermore, defects of Ba(1) at $z = 0.0$ and Ba(2) at $z = 0.5$ were indicated. As previously reported (*5*), electron microscopy revealed the nonequivalency of Ba–O layers at $z = 0.0$ and at $z = 0.5$, so the starting model was modified by decreasing the occupancy of Ba(1) at $z = 0.0$. By this treatment, the model lost centrosymmetry and successive Fourier syntheses indicated the addition of atoms at ($\frac{2}{3}$, $\frac{1}{3}$, 0.24) and (0.85, 0.15, 0.07) more clearly. We assumed the former to be an inside-spinel Ba (and/or Pb) ion and the latter to be an interstitial Al ion as was found in barium β-alumina (*6*). In addition, Al(1) at $z = 0.15$ showed a little deficiency. Using an overall temperature factor, the refinement was accomplished on the modified model, with reduction of an R value to 0.141. At this stage, difference Fourier maps still indicated another additional electron density at ($\frac{2}{3}$, $\frac{1}{3}$, 0.22), which we supposed to be another inside-spinel large cation site. So we placed a Ba ion at this site with little occupancy in the next refinement. The R value dropped to 0.101. The difference Fourier synthesis at the R value of 0.101 still pointed out a small shift from the theoretical position of Ba(1) and Ba(2). The simultaneous change of coordinations and occupancies of Ba(1) and Ba(2) with other parameters met with failure in the least-squares refinement because of the high correlations between these parameters. So, refinement was attempted by changing only one or two of the parameters at the same time, while the other parameters remained fixed. After the addition of O(11), which is bonded to interstitial Al ion pair after the Reidinger defect mechanism (*7*), individual isotropic temperature factors were introduced. Because the difference Fourier maps still indicated the split of Al(5), O(9), and O(10) atoms, refinement with these splitting atoms was further conducted step by step. Finally, all parameters were varied simultaneously with an R value of 0.036 ($wR = (\Sigma w(|F_o| - |F_c|)^2/\Sigma w|F_o|^2)^{1/2} = 0.040$, $w = 1.0$). At this stage, elongated electron density just below O(3) at $z = 0.108$ was observed in the difference Fourier map, which we attributed to a partial shift of O(3). After the addition of O(12) at the site just below O(3), the final refinement with varying all parameters converged to $R = 0.030$ ($wR = 0.034$, $w = 1.0$). The final difference Fourier maps showed random peaks and depressions not exceeding the range of -1.1 to $+0.7$ eÅ^{-3}. Anisotropic refinement was not attempted because there would be too many parameters compared with the number of observed diffraction data. Since the specimen contains

about 20% Pb instead of Ba, the Pb ion should be included in the refinement procedure. For the reason to be described in the next section, Ba(4) was assumed to be the site where large amount of Pb was concentrated. After changing Ba(4) into Pb, the refinement gave a total number of Ba and Pb as 2.27, which is in good agreement with the value of 2.34 deduced from EPMA data, lattice parameters, and density (*5*). The *R* value did not change after these treatments.

As previously mentioned, there is another possibility of having space group symmetry $P\bar{6}m2$. The intensities *hkl* and *khl* were observed to have almost the same value, and, furthermore, the result of $P\bar{6}$ refinement showed that the *y* coordinates were almost twice those of *x*. These facts indicate the space group $P\bar{6}m2$, of higher symmetry. The isotropic refinement using 432 independent reflections results in $R = 0.030$ ($wR = 0.033$, $w = 1.0$) when adopting $P\bar{6}m2$ symmetry. No significant change in the coordinates and occupancies was observed; also, the *R* value remained almost unchanged. Accordingly we adopted $P\bar{6}m2$ as the space group symmetry for barium β(II)-alumina as well as barium lead β(II)-alumina.

The atomic coordinates are shown in Table II. Tables III and IV contain the interatomic distances and bond angles, respectively.

TABLE II

THE POSITIONAL[a] AND THERMAL PARAMETERS

Atom	Position	Number per unit cell	*x*	*z*	*B*[b]
Ba(1)	3*j*	0.685(10)	0.6770(12)	0	0.73(7)
Ba(2)	3*k*	1.002(10)	0.3202(6)	$\frac{1}{2}$	0.51(5)
Ba(3)	2*i*	0.211(19)	$\frac{2}{3}$	0.2202(6)	0.35(21)
Pb	2*i*	0.375(9)	$\frac{2}{3}$	0.2422(2)	0.42(6)
Al(1)	6*n*	3.96(7)	0.8351(8)	0.1515(2)	0.35(7)
Al(2)	6*n*	6	0.1660(6)	0.3573(1)	0.34(3)
Al(3)	2*h*	2	$\frac{1}{3}$	0.2302(3)	0.44(8)
Al(4)	2*i*	1.48(5)	$\frac{2}{3}$	0.2767(3)	0.54(15)
Al(5)	6*n*	1.99(6)	0.3084(9)	0.0741(3)	0.20(16)
Al(6)	2*i*	2	$\frac{2}{3}$	0.4249(2)	0.26(7)
Al(7)	2*g*	2	0	0.2532(3)	0.18(6)
Al(8)[c]	6*n*	1.90(8)	0.8565(10)	0.0694(3)	0.19(16)
O(1)	6*n*	6	0.1607(12)	0.2062(3)	0.86(10)
O(2)	6*n*	6	0.8460(10)	0.3048(2)	0.50(9)
O(3)	6*n*	4.76(18)	0.5053(16)	0.1080(4)	0.84(18)
O(4)	6*n*	6	0.4942(11)	0.3996(3)	0.53(10)
O(5)	2*i*	1.86(18)	$\frac{2}{3}$	0.2004(10)	0.64(26)
O(6)	2*h*	2	$\frac{1}{3}$	0.3102(5)	0.46(16)
O(7)	2*g*	2	0	0.1131(5)	0.29(17)
O(8)	2*g*	2	0	0.3962(5)	0.33(16)
O(9)	3*j*	1.18(10)	0.261(4)	0	2.3(8)
O(10)	3*k*	1	0.686(4)	$\frac{1}{2}$	0.40(42)
O(11)[c]	3*j*	0.99(10)	0.916(4)	0	1.1(6)
O(12)	6*n*	1.67(18)	0.494(3)	0.0827(9)	0.23(37)

[a] $y = 2x$.
[b] Isotropic temperature factor (Å^2).
[c] Interstitials.

Discussion

In the previous paper (*5*), we supposed the structure of barium β(II)-alumina to be essentially of a β-Al_2O_3 type on the basis of chemical formula $Ba_{2.34}Al_{21.0}O_{33.84}$, and assumed that an "excess Ba–O layer" containing 1.33 Ba per mirror plane and a "fully occupied Ba–O layer" containing 1.0 Ba would stack alternately, separated by a spinel block. The model of Zandvergen *et al.* (*8*) is essentially a variation of our model, though a more elaborate one. Indeed the refined parameters clearly indicate isostructural barium lead β(II)-alumina to be of a β-Al_2O_3 structure, but the number of Ba ions in a mirror plane per single unit cell does not exceed 1.0, which invalidates the concept of "excess Ba–O layer." Instead, there are two types of mirror planes, i.e., a defect Ba–O layer ($z = 0.0$) and a fully occupied Ba–O layer ($z = 0.5$). The latter layer contains no defects or interstitials in its neighborhood. These layers stack alternately being separated by a spinel block. Furthermore, excess Ba(Pb) ions were found inside the spinel blocks; the existence of "inside-spinel" sites seems to be very different from most other β-Al_2O_3 compounds. Only a few cases of inside-spinel sites occupied by a large cation have been reported (*16, 17*). For the β-gallate system, it was observed that excess Na^+ in sodium β-gallate substitutes for Ga^{3+} inside the spinel block, forming a Na^+ tetrahedron

TABLE III

INTERATOMIC DISTANCES

		Number of bonds	Distance (Å)
	Octahedral coordination		
Al(1)	–O(1)	2	2.017(11)
	–O(3)	2	1.886(14)
	–O(5)	1	1.982(15)
	–O(7)	1	1.826(9)
Al(2)	–O(2)	2	1.966(9)
	–O(4)	2	1.865(10)
	–O(6)	1	1.949(8)
	–O(8)	1	1.841(8)
Al(7)	–O(1)	3	1.895(11)
	–O(2)	3	1.905(9)
	Tetrahedral coordination		
Al(3)	–O(1)	3	1.763(12)
	–O(6)	1	1.833(13)
Al(4)	–O(2)	3	1.854(10)
	–O(5)	1	1.748(24)
Al(5)	–O(3)	2	1.744(18)
	–O(9)	1	1.759(12)
	–O(12)	1	1.810(28)
Al(6)	–O(4)	3	1.771(10)
	–O(10)	1	1.731(6)
Al(8)	–O(7)	1	1.715(11)
	–O(11)	1	1.694(15)
	–O(12)	2	1.790(24)
(	–O(3)	2	1.93(2))
	Polyhedron 9-coordinated		
Ba(1)	–O(3)	6	2.931(13) (averaged)
	–O(9)	3	2.95(4) (averaged)
Ba(2)	–O(4)	6	2.783(9) (averaged)
	–O(10)	3	3.14(4) (averaged)
	Inside-spinel site		
Ba(3)	–O(1)	6	2.819(10)
	–O(2)	3	2.604(13)
	–O(12)	3	3.570(26)
(	–O(3)	3	3.011(16))
Pb	–O(1)	6	2.920(10)
	–O(2)	3	2.255(9)
(	–O(3)	3	3.450(12))

(*17*). But this may not be the case with barium β(II)-alumina or barium lead β(II)-alumina as the radius of the Ba^{2+} ion (1.36 Å) or the Pb ion (1.18 Å) (*18*) is very large compared with that of the Al^{3+} ion (0.53 Å) (*18*) in the spinel block. So another mechanism might operate in this case. The peculiar defects of barium β(II)-alumina described below afford a clue to the inside-spinel site formation.

In barium β-alumina (*6*), interstitial Al and oxygen ions due to the Reidinger defects were observed. The same interstitial Al ion at $z = 0.07$ and oxygen ion in the $z = 0.0$ mirror plane were found. The fact that the number of atoms per unit cell of intersti-

TABLE IV

BOND ANGLES

		Bond angles (°)
	Octahedral coordination	
O(1)	–Al(1)–O(1)′	84.04(62)
	–O(3)	91.78(58)
	–O(5)	89.05(54)
	–O(7)	86.76(56)
O(3)	–Al(1)–O(3)′	91.92(88)
	–O(5)	85.82(70)
	–O(7)	98.08(55)
O(2)	–Al(2)–O(2)′	82.31(52)
	–O(4)	92.29(44)
	–O(6)	91.54(33)
	–O(8)	85.03(39)
O(4)	–Al(2)–O(4)′	92.84(62)
	–O(6)	84.91(40)
	–O(8)	98.21(40)
O(1)	–Al(7)–O(1)′	90.88(44)
	–O(2)	91.73(36)
O(2)	–Al(7)–O(2)′	85.54(39)
	Tetrahedral coordination	
O(1)	–Al(3)–O(1)′	110.72(31)
	–O(6)	108.19(32)
O(2)	–Al(4)–O(2)′	108.63(27)
	–O(5)	110.30(26)
O(3)	–Al(5)–O(3)′	111.87(62)
	–O(9)	110.0(15)
	–O(12)	106.8(9)
O(9)	–Al(5)–O(12)	111.2(14)
O(4)	–Al(6)–O(4)′	109.80(27)
	–O(10)	105.9(11)
O(7)	–Al(8)–O(11)	105.7(14)
	–O(12)	110.8(10)
O(11)	–Al(8)–O(12)	110.6(13)
O(12)	–Al(8)–O(12)′	108.2(17)
O(3)	–Al(8)–O(11)	128.1(9)

tial Al(8) at $z = 0.07$ is almost the same as the number of defect atoms at the Al(1) site ($z = 0.15$) and twice as much as that of interstitial O(11) in the mirror plane indicates that the defect mechanism is of a Reidinger type. In barium β-alumina, the Reidinger defect occurs singly. In other words, only one of three Al(1) sites ($z = 0.15$) becomes vacant with creation of an interstitial Al(8) according to the Frenkel defect mechanism and a pair of the interstitial Al(8) ions was bridged by an interstitial oxygen in the mirror plane (Fig. 1a). These interstitials create a Ba vacancy in the $z = 0.0$ mirror plane. Accordingly, the sum of the number of Ba and interstitial oxygens for one mirror plane of a single unit cell becomes unity in this case. On the other hand, in the case of barium lead β(II)-alumina, it sums up to about 1.68, which is significantly larger than 1.0. Since Ba or Pb cannot coexist with interstitial Al and oxygen in the same mirror plane of a single unit cell from the viewpoint of ionic radius, it follows that the Reidinger defects should occur in multiple state in a mirror plane at $z = 0.0$ of a single unit cell. On the assumption that the Reidinger defects occur triply, the occupancy of the atoms in the $z = 0.0$ mirror plane can be explained well. We would like

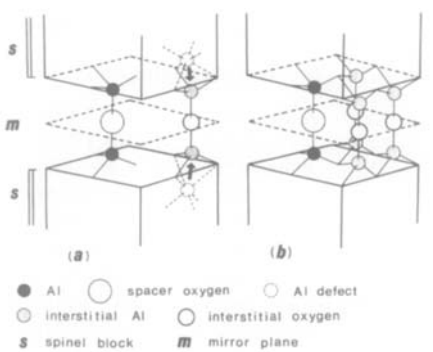

FIG. 1. (a) The Reidinger defect. The bold arrows indicate the shift of Al ions after the Frenkel defect mechanism. (b) "Triple Reidinger defects": In this case, the Reidinger defects take place triply in a mirror plane of a single unit cell. For simplification, Al vacancies are not shown in the (b).

to refer to this type of defect as "the triple Reidinger defects." As shown in Fig. 1b, the interstitial oxygen O(11) ions are so crowded that electrostatic repulsion may cause the displacement from the ideal mid-oxygen (mO) site ($\frac{5}{6}$, $\frac{2}{3}$, 0.0) toward the anti-BR site (0.0, 0.0, 0.0). In addition to interstitial oxygens, interstitial Al(8) also shifts a little from the ideal site ($\frac{5}{6}$, $\frac{2}{3}$, 0.07) to (0.0, 0.0, 0.07), causing a partial shift of O(3) to O(12). Al(8) makes bonds to two O(12) and O(7) as well as O(11) forming a nondistorted tetrahedron.

Defects are not confined to these atoms but also exhibited in Al(4) and O(5) within the spinel block. The fact that occupancy of Al(4) of 0.74 is almost the same as that of Al(1) suggested to us the occurrence of the simultaneous defect of Al(4) and Al(1). In the case of Al(4) and Al(1) defects, O(5) remains surrounded by 12 oxygens as the nearest neighbors at a distance of about 2.8 Å. Thus it is reasonable to assume that O(5) also becomes vacant simultaneously with Al(4) and Al(1). As shown in Table II, however, the occupancy of O(5) is not consistent with this assumption. Probably this discrepancy can be attributed to the large electron density of Ba(3) ion at $z = 0.220$ which, in the average structure, effects the occupancy of O(5) at $z = 0.200$. The combination of the triple Reidinger defects and inside-spinel defects forms a 12-coordinated polyhedral site in the spinel block as shown in Fig. 2, the site that Ba(Pb) ions occupy. In conclusion, the triple Reidinger defects together with Al(4) and O(5) defects produce a large 12-cornered polyhedral site inside the spinel block, where large cations such as Ba and/or Pb are situated. Such an inside-spinel site has not been reported up to now.

The remaining problem is the species of the cation and the ratio of Pb/Ba at each large cation site. As the occupancy is varied at each large cation site in the refinement, the Pb/Ba ratio at each site cannot be

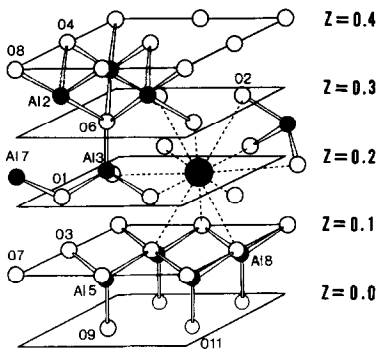

FIG. 2. A schematic depiction of the "inside-spinel site" which is formed by the triple Reidinger defects followed by the defects of Al(4) and O(5). A large filled circle represents a Ba (or Pb) ion at the inside-spinel site, and small ones are Al ions. Oxygen ions are shown by open circles. O(11) and Al(8) are interstitials.

determined exactly by the least-squares calculation. We noted that there exist two distinct inside-spinel sites, ($\frac{2}{3}$, $\frac{1}{3}$, 0.22) and ($\frac{2}{3}$, $\frac{1}{3}$, 0.24). The latter site may as well be called the "9-coordinated polyhedral site" rather than the "distorted" 12-coordinated polyhedral site. Here we supposed that the large cation sites of ($\frac{2}{3}$, $\frac{1}{3}$, 0.22) and ($\frac{2}{3}$, $\frac{1}{3}$, 0.24) are attributable to Ba and Pb ions, respectively. This assumption is based on the following reasons; At the site ($\frac{2}{3}$, $\frac{1}{3}$, 0.24), the distance to the nearest oxygen O(2) is only 2.3 Å, which is too short for the large Ba–O distance of about 2.8–3.0 Å (*6*). It would be better to assume that the smaller Pb ion might be situated at this site ($\frac{2}{3}$, $\frac{1}{3}$, 0.24). The refinement was accomplished on this assumption with the result that total number of Ba and Pb cations per unit cell is 2.27, which is in good agreement with the value of 2.34 deduced from EPMA, density, and lattice parameters. The ratio Pb/Ba becomes about 0.20, which is only a little smaller than the previously reported value of 0.25. So, it may be that Pb ions are concentrated at the site ($\frac{2}{3}$, $\frac{1}{3}$, 0.24), although a small amount of Pb ions might substitute for Ba ions at the other site.

On the basis of the atomic parameters of the average structure and defect mechanism discussed above, we can propose a structure model for barium lead β(II)-alumina after the method used for elucidation of the structure of barium β-alumina (*6*) and rare-earth hexaaluminates (*19, 20*). Because simultaneous occupation of the Ba ion, and interstitial Al and O ions is not possible in the same mirror plane of a single unit cell, we can assume at least two types of unit cells in barium lead β(II)-alumina as shown in Figs. 3a and b. In one kind of unit cell, one Ba ion is situated near the BR site at z = 0.0, so the composition is "$Ba_2Al_{22}O_{34}$" with charge of +2. This cell contains no defects and shows an ideal formula of β-alumina ($MAl_{11}O_{17}$, where M = large cation). In contrast, defect of a Ba ion at z = 0.0, the triple Reidinger defects, and defects of Al(4) and O(5) take place in the other

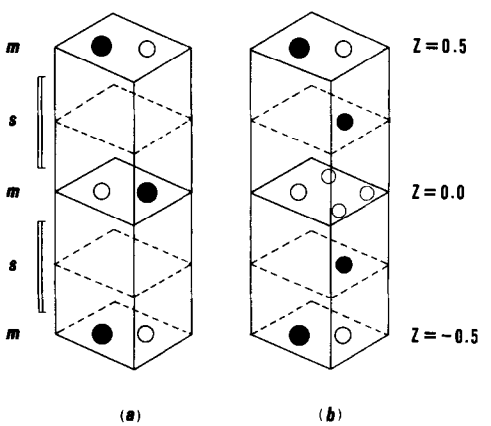

FIG. 3. Simplified models representing two kinds of unit cells assumed to constitute the structure of barium (lead) β(II)-alumina. Filled circles indicate large cations Ba (or Pb), and oxygen ions are shown by open circles. "S" and "M" are abbreviations for "spinel block" and "mirror plane," respectively. (a) Unit cell containing a Ba and an oxygen ion in each mirror plane. This cell is free from any defects (i.e., 'perfect cell'), and has a formula "$Ba_{2.0}Al_{22.0}O_{34.0}$." (b) Unit cell containing Ba (or Pb) ions at the inside-spinel sites and interstitials due to the triple Reidinger defects. Interstitial ions cause a Ba vacancy at the large cation site (z = 0.0). This "defect cell" has a formula "$Ba_{3.0}Al_{20.0}O_{35.0}$."

kind of unit cell, the composition of which becomes "$(BaPb)_3Al_{20}O_{35}$" with the charge of −4. As there is no evidence for other types of cells, we supposed that these perfect and defect cells constitute barium lead β(II)-alumina. These cells are not electrostatically neutral, so the ratio for perfect cell to defect cell would be 2 to 1. The comparison of the occupancy deduced from the structure model and the refined parameters are given in Table V. These data are in good agreement except for O(5) probably for the reason already described in this section. The resulting chemical formula "$(BaPb)_{2.33}Al_{21.33}O_{34.33}$" based on the model is very near to the formula "$(Ba_{0.8}Pb_{0.2})_{2.34}Al_{21.00}O_{33.84}$" obtained by using EPMA, lattice parameters, and density data. This structural model can be directly applied to pure barium β(II)-alumina. Furthermore, it seems that this peculiar structure is not confined to barium β(II)-alumina. Zandvergen *et al.* (8) reported the compound "$1.31BaO \cdot 6Ga_2O_3$," and presented its structure image, which resembled that obtained for barium β(II)-alumina by using high-resolution electron microscopy (*12*). Probably barium β(II)-alumina and "$1.31BaO \cdot 6Ga_2O_3$" are isostructural compounds.

TABLE V

COMPARISON OF THE SITE OCCUPANCY

Atom	Number of atoms per unit cell: Result of refinement	Model
Ba(1)	0.685(10)	0.667
Ba(2)	1.002(10)	1.000
Ba(3)	0.211(19)	0.20
Pb	0.375(9)	0.467
Al(1)	3.96(7)	4.00
Al(4)	1.48(5)	1.33
Al(5)	1.99(6)	2.00
Al(8)	1.90(8)	2.00
O(3)	4.76(18)	4.00
O(5)	1.86(18)	1.33
O(9)	1.18(10)	1.00
O(11)	0.99(10)	1.00
O(12)	1.67(18)	2.00

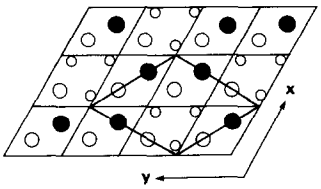

FIG. 4. A schematic representation of the two-dimensional superstructure cells in the $z = 0.0$ mirror planes. Filled circles indicate Ba ions, large open circles represent spacer oxygens O(9), and small open circles are interstitial O(12) ions. The outlines of the $a\sqrt{3} \times a\sqrt{3}$ superstructure are indicated by heavy lines.

The structural model described above is readily applicable to explain the intergrowth phenomenon reported in Refs. (*9, 10*), and the presence of "APB" (*5, 8*) and the superstructure. The $a\sqrt{3} \times a\sqrt{3}$ superstructure is very characteristic of β(II)-alumina compounds, and has been observed by several researchers (*5, 9, 10*). This superstructure can be attributed to these three cells (two perfect cells and one defect cell), which form a large unit cell as shown in Fig. 4. In the figure the defect cells are so arranged as not to be adjacent to each other. The diffuse reflections along c^* axis observed previously (*5, 9, 10*) can also be explained by assuming that there are almost no correlations between the defect Ba–O layers in arrangement of the mirror planes containing the interstitial oxygen ions.

The problem of the intergrowth can be also clearly solved. The intergrowth between barium β-alumina and barium β(II)-alumina was observed in the sintered specimens (*9, 10*). We also observed it in the crystal boules grown by using the intermediate composition as the starting materials. In the previous paper (*6*), we revealed barium β-alumina to be composed of a fully occupied half cell "$BaAl_{11}O_{17}$" and a defect half cell "$OAl_{11}O_{17}$." The former is also the

component of barium β(II)-alumina. The presence of the cell, common to these two compounds, would be the reason for the intergrowth between barium β-alumina and barium β(II)-alumina, formed probably under the inhomogeneous growth conditions. In Fig. 5, the intergrowth between them is depicted.

Another problem concerns "APB." We have mentioned the boundary shown in Fig. 3 of Ref. (*5*) as "APB" (antiphase boundary) with a displacement vector of $\frac{1}{2}c$. Indeed, when only two kinds of BaO layers are taken into consideration, this nomenclature may not be wrong, but spinel blocks do not fit with those which have migrated by $\frac{1}{2}c$. It would be reasonable to think that the coherency of the spinel block is preserved across the "APB." Accordingly we would rather consider the boundary to be a twin boundary instead of APB. Twins are related by glide reflection in the (100) plane. Between twins, the *c* axis is held in common, and the *a* and *b* axes are placed in parallel but opposite directions. From the viewpoint of the origin, it may be a growth twin, and, from the viewpoint of the axial relations, it would be called a "coaxial twin" (*21*). As long as the size of twin domain is large, the intensities of X-ray reflections would not be influenced by twinning. The schematic representation of twin model is given in Fig. 6.

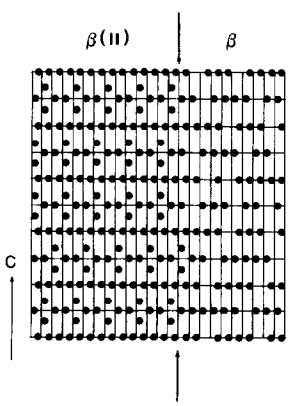

FIG. 5. The intergrowth between barium β-alumina ("β") and barium β(II)-alumina ("β(II)"). Black circles represent Ba ions. Other ions are omitted.

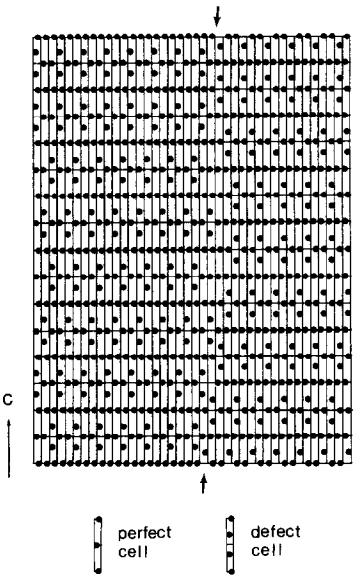

FIG. 6. The model of twinning in barium β(II)-alumina. Black circles are Ba ions in the mirror planes and inside spinel blocks. Arrows show the boundary.

We now try to confirm the intergrowth and twin models as well as the structure model by using high-resolution electron microscopy and computer simulation of the images.

Acknowledgments

The authors are indebted to Dr. Y. Bando for reading the manuscript and for his helpful suggestions.

References

1. F. HABEREY, G. OEHLSCHLEGEL, AND K. SAHL, *Ber. Dtsch. Keram. Ges.* **54,** 373 (1977).
2. S. KIMURA, E. BANNAI, AND I. SHINDO, *Mater. Res. Bull.* **17,** 209 (1982).
3. N. IYI, S. TAKEKAWA, AND S. KIMURA, *J. Solid State Chem.* **59,** 250 (1985).
4. F. P. F. VAN BERKEL, H. W. ZANDBERGEN, G. C. VERSHOOR, AND D. J. W. IJDO, *Acta Crystallogr. C* **40,** 1124 (1984).

5. N. IYI, S. TAKEKAWA, Y. BANDO, AND S. KIMURA, *J. Solid State Chem.* **47,** 34 (1983).
6. N. IYI, Z. INOUE, S. TAKAKAWA, AND S. KIMURA, *J. Solid State Chem.* **52,** 66 (1984).
7. W. L. ROTH, F. REIDINGER, AND S. LAPLACA, *in* "Superionic Conductors" (G. D. Mahan and W. L. Roth, Eds.), p. 223, Plenum, New York (1977).
8. H. W. ZANDBERGEN, F. C. MIJLHOFF, D. J. W. IJDO, AND G. VAN TENDELOO, *Mater. Res. Bull.* **19,** 1143 (1984).
9. P. E. D. MORGAN AND T. M. SHAW, *Mater. Res. Bull.* **18,** 539 (1983).
10. N. YAMAMOTO AND M. O'KEEFFE, *Acta Crystallogr. B* **40,** 21 (1984).
11. S. TAKEKAWA, *in* "Research Report of NIRIM," **37,** pp. 15–17, NIRIM (1983).
12. Y. BANDO, private communication (1984).
13. T. SAKURAI, K. NAKATSU, H. IWASAKI, AND M. FUKUHARA, RSFLS-4, UNICS II, Crystallogr. Soc. Japan (1967).
14. T. SAKURAI, RSSFR-5, UNICS II, Crystallogr. Soc. Japan (1967).
15. C. R. PETERS, M. BETTMAN, J. W. MOORE, AND M. D. GLICK, *Acta Crystallogr. B* **27,** 1826 (1971).
16. W. L. ROTH, *Trans. Amer. Crystallogr. Assoc.* **11,** 51 (1975).
17. M. P. ANDERSON, L. M. FOSTER, AND S. J. LAPLACA, *Solid State Ionics* **5,** 211 (1981).
18. R. D. SHANNON AND C. T. PREWIRT, *Acta Crystallogr. B* **25,** 925 (1969).
19. N. IYI, Z. INOUE, S. TAKEKAWA, AND S. KIMURA, *J. Solid State Chem.* **54,** 70 (1984).
20. N. IYI, Z. INOUE, AND S. KIMURA, *J. Solid State Chem.* **54,** 123 (1984).
21. Y. TAKANO, "Classification of Twins," p. 57, Kokon Shoin, Tokyo (1973).